Stem Cell Reports
Article

OPEN ACCESS

A Chemical Biology Study of Human Pluripotent Stem Cells Unveils HSPA8 as a Key Regulator of Pluripotency

Yijie Geng,[1,*] Yongfeng Zhao,[2] Lisa Corinna Schuster,[1] Bradley Feng,[1] Dana A. Lynn,[1] Katherine M. Austin,[1] Jason Daniel Stoklosa,[1] and Joseph D. Morrison[1]

[1]Department of Cell and Developmental Biology, University of Illinois at Urbana-Champaign, Urbana, IL 61801, USA
[2]Stem Cell Center, Department of Bioengineering, University of California, Riverside, Riverside, CA 92521, USA
*Correspondence: geng2@illinois.edu
http://dx.doi.org/10.1016/j.stemcr.2015.09.023

SUMMARY

Chemical biology methods such as high-throughput screening (HTS) and affinity-based target identification can be used to probe biological systems on a biomacromolecule level, providing valuable insights into the molecular mechanisms of those systems. Here, by establishing a human embryonal carcinoma cell-based HTS platform, we screened 171,077 small molecules for regulators of pluripotency and identified a small molecule, Displurigen, that potently disrupts hESC pluripotency by targeting heat shock 70-kDa protein 8 (HSPA8), the constitutively expressed member of the 70-kDa heat shock protein family, as elucidated using affinity-based target identification techniques and confirmed by loss-of-function and gain-of-function assays. We demonstrated that HSPA8 maintains pluripotency by binding to the master pluripotency regulator OCT4 and facilitating its DNA-binding activity.

INTRODUCTION

The pluripotency regulators OCT4, NANOG, and SOX2 form a core transcription regulatory network through auto- and reciprocal activations at the transcription level, which is believed to be responsible for the maintenance of human embryonic stem cell (hESC) pluripotency (Boyer et al., 2005). At the same time, multiple protein factors belonging to a diversity of functional categories, such as transcription factors, epigenetic factors, and signaling components, work cooperatively to form an expanded pluripotency factor network that supports the core pluripotency network (Boyer et al., 2005). In contrast to the well-defined core network, our knowledge of this expanded pluripotency network, including its components, the interactions between these components, and the mechanism of interaction between the expanded network and the core network, remains insufficient.

Bioactive small molecules have been applied to the field of hESC research with success. Many such studies have applied small molecules as modulators of lineage-specific differentiations (Borowiak et al., 2009; Chen et al., 2009, 2012; Gonzalez et al., 2011a; Lian et al., 2012; Mahmood et al., 2010). Other studies have exploited small molecules as chemical probes to uncover novel molecular mechanisms underlying hESC pluripotency or differentiation (Chen et al., 2006; Xu et al., 2010; Zhu et al., 2009). High-throughput screenings (HTS) were usually conducted for the search of such molecules. If the mechanism of action was unknown for a given molecule, affinity-based target identification methods can be used to identify its biological target(s). These studies have been used to identify novel protein factors and to unveil previously unknown molecular mechanisms that regulate hESC fate determination (Xu et al., 2008).

In recent years, hESCs and human induced pluripotent stem cells (hiPSCs) have been used successfully for HTS in several studies (Barbaric et al., 2010; Ben-David et al., 2013; Desbordes et al., 2008; Gonzalez et al., 2011b; Kameoka et al., 2014; Kumagai et al., 2013; Manganelli et al., 2014; Xu et al., 2010). However, the high cost associated with the maintenance and scale-up of human pluripotent stem cells (hPSCs) inevitably limits the scale of their application in HTS studies. We chose to explore an alternative source of pluripotent stem cells, human embryonal carcinoma cells (hECCs), as a robust platform for HTS with low cost. hECCs are pluripotent stem cells derived from human teratocarcinomas and are considered to be the malignant counterparts of hESCs. The molecular regulatory mechanism of hECC pluripotency has been shown to mimic that of hESCs (Josephson et al., 2007). Because of their cancerous nature, hECCs are not prone to spontaneous differentiation and require a less demanding culture condition compared with hPSCs. Experimental results acquired from studies using hECCs have been proven to be highly stable and readily reproducible (Josephson et al., 2007), making hECCs ideal candidate platforms for HTS purposes.

Based on the concept of hECC-based HTS, we established a pluripotency reporter system using the hECC line NTERA-2. Using this system, we conducted a large-scale chemical screening and found 122 small molecules that disrupt hESC pluripotency. One of these molecules, which we named Displurigen, potently disrupts hESC pluripotency by targeting heat shock 70-kDa protein 8 (HSPA8,

the constitutively expressed member of the 70-kDa heat shock protein family), as discovered using affinity-based target identification methods and functional validations. We demonstrated that HSPA8 helps maintain pluripotency by direct binding to the OCT4 protein and facilitating OCT4 binding to DNA.

RESULTS

Establishment of an NTERA-2 Cell-Based Pluripotency Reporter System

To avoid high experimental variations associated with hESC-based HTS platforms, we established an HTS platform using the hECC line NTERA-2. NTERA-2 is a clonal subline of TERA-2, one of the first established hECC lines (Andrews et al., 1984). NTERA-2 cells are able to differentiate into all three germ layers in vivo in the form of teratocarcinomas. In culture, these cells differentiate in response to several inducers of differentiation, most notably retinoic acid (RA) (Andrews, 1984), hexamethylene bis-acetamide (HMBA) (Andrews et al., 1986, 1990), and bone morphogenetic protein 7 (Andrews et al., 1994). These agents also induce differentiation of hESCs (Draper et al., 2002; Xu et al., 2002; zur Nieden et al., 2005). Furthermore, basic fibroblast growth factor (bFGF) helps maintain the pluripotent state of both NTERA-2 cells and hESCs (Andrews et al., 1984; Thomson et al., 1998). The similarities in their responses toward external factors indicate that NTERA-2 cells and hESCs have very similar molecular mechanisms governing their respective pluripotent states.

An NTERA-2 cell-based reporter cell line was constructed by stable integration of an EGFP reporter gene driven by a 4-kb OCT4 promoter (Gerrard et al., 2005). EGFP-positive cells were selected by flow cytometry after drug selection. The selected stable cell line nearly homogeneously expressed EGFP and maintained this expression after multiple (more than 20) rounds of passaging (Figure 1A). This reporter line is hereafter referred to as NTERA-2-OP4k, with "OP4k" referring to the 4-kb OCT4 promoter. To test the response of this reporter system to known external regulators of pluripotency, NTERA-2-OP4k cells were cultured at low density and incubated with known inhibitors of pluripotency, including RA and HMBA, and with an enhancer of pluripotency, bFGF, for 6–7 days. The Rho-associated coiled coil-containing protein kinase (ROCK) inhibitor Y-27632 was also tested as a cell survival enhancer (Watanabe et al., 2007). RA and HMBA dramatically reduced the cellular EGFP signal, as shown by fluorescence-activated cell sorting (FACS) analysis and fluorescent imaging (Figure 1B; Figure S1A). This was accompanied by a dramatic downregulation of the endogenous protein expression of OCT4, as shown by western blotting (Figure S1B). On the other hand, in bFGF- and Y-27632-treated cells, EGFP expression and the endogenous expression of OCT4 remained largely unaltered compared with the DMSO control (Figure 1B; Figure S1). These results demonstrate that the EGFP expression of NTERA-2-OP4k reporter cells is regulated by known regulators of pluripotency in the same way as the expression of endogenous OCT4 and indicate that the OCT4-EGFP reporter signal faithfully reflects the endogenous expression of OCT4 and the pluripotency state of the cells.

NTERA-2-OP4k Cell-Based HTS Identified Small Molecule Regulators of Pluripotency

Before applying the NTERA-2-OP4k reporter system to HTS, we first verified whether the responses of the OCT4-EGFP reporter could be accurately measured under HTS conditions. For this test, NTERA2-OP4k cells were seeded at low densities ($0.1–0.25 \times 10^5$ cells/cm^2) in 96-well plates. Pluripotency and survival regulators, including RA, HMBA, bFGF, and Y-27632, were added immediately following cell plating. Cells were incubated for 6–7 days without medium change and then scanned for EGFP signals using a fluorescence plate reader. As a result, cells treated with the pluripotency inhibitors RA and HMBA showed significantly decreased EGFP signals, whereas bFGF- and Y-27632-treated cells maintained high levels of EGFP signals compared with the DMSO control (Figure 1C). This result is consistent with the results obtained previously by FACS analysis and fluorescence imaging in non-HTS settings (Figure 1B; Figure S1A), confirming the validity of using NTERA-2-OP4k as a pluripotency reporter line for HTS.

For HTS, 171,077 small molecules with diverse chemical structures were screened using the NTERA-2-OP4k reporter cell-based platform. These molecules were hosted by the University of Illinois at Urbana-Champaign (UIUC) HTS facility in four chemical libraries. For the screen, NTERA-2-OP4k cells were seeded at low densities in 96- or 384-well plates and incubated with screening compounds and DMSO controls (included in all screening plates), added using pin tools immediately after seeding, at the final concentrations described in the Supplemental Experimental Procedures. Cells were kept in a 37°C incubator for 6–7 days without medium change and then scanned for EGFP signal intensities using a fluorescence plate reader. Wells with EGFP intensities lower than 70% of the average EGFP intensity of the DMSO controls (average level of background signals subtracted before comparison) in the same plates were identified as candidate hits.

We expect two types of compounds to produce false positives by reducing EGFP signal intensities in the treated wells without inducing cellular differentiation. These include cytotoxic or apoptosis-inducing compounds that caused cell death (Figure 1D, Cell Death) and compounds that inhibited cell proliferation (Figure 1D, Reduced

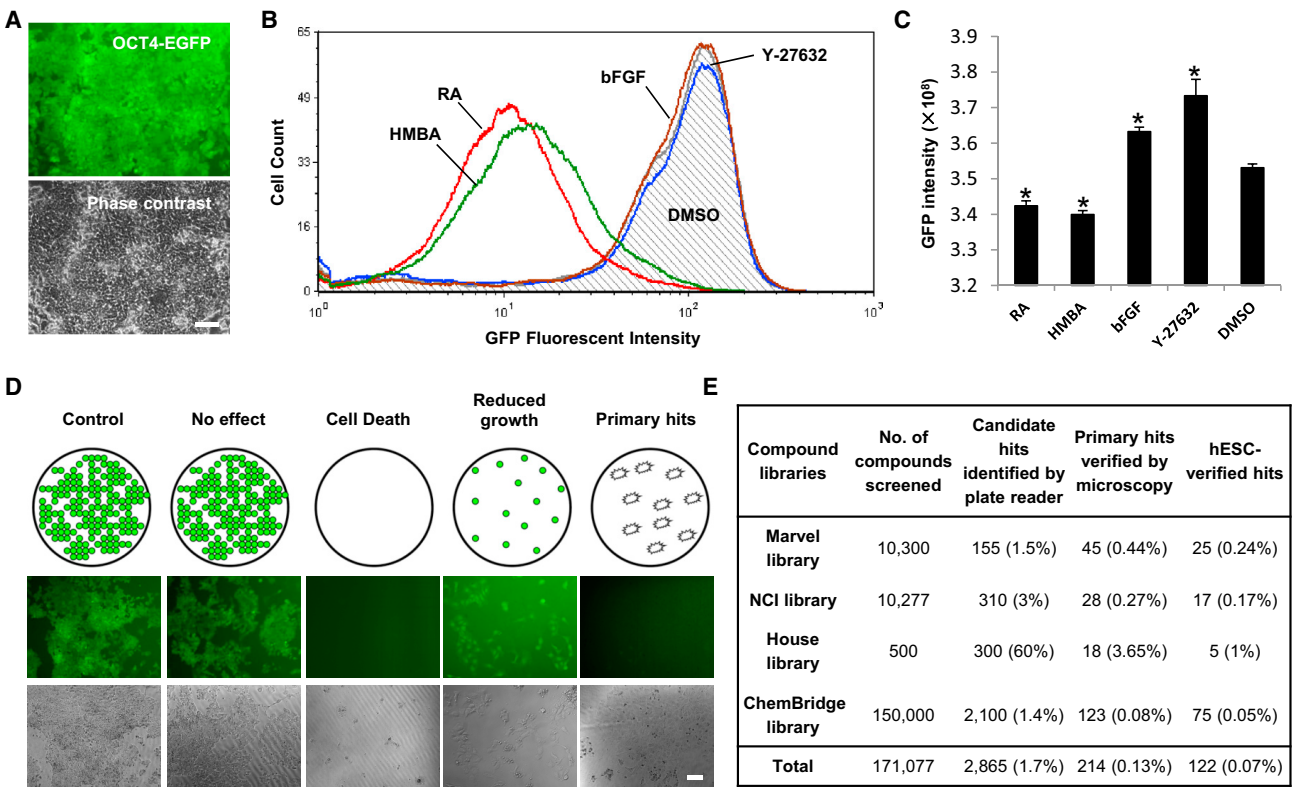

Compound libraries	No. of compounds screened	Candidate hits identified by plate reader	Primary hits verified by microscopy	hESC-verified hits
Marvel library	10,300	155 (1.5%)	45 (0.44%)	25 (0.24%)
NCI library	10,277	310 (3%)	28 (0.27%)	17 (0.17%)
House library	500	300 (60%)	18 (3.65%)	5 (1%)
ChemBridge library	150,000	2,100 (1.4%)	123 (0.08%)	75 (0.05%)
Total	171,077	2,865 (1.7%)	214 (0.13%)	122 (0.07%)

Figure 1. Establishment of an NTERA-2-OP4k Reporter Cell-Based HTS System and General Outcome of the Screen

(A) Fluorescent (top) and phase contrast (bottom) images of NTERA-2-OP4k cells. Scale bar, 100 μm.

(B) Histogram of GFP expression in NTERA-2-OP4k cells analyzed by flow cytometry. Cells were treated with DMSO, Y-27632 (10 μM), bFGF (4 ng/ml), RA (10 μM), and HMBA (3 mM) for 6 days.

(C) Quantification of GFP intensity after treatment of NTERA-2-OP4k cells with DMSO, Y-27632, bFGF, RA, and HMBA for 6 days. Cells were cultured in the 96-well plate format. GFP intensity was determined using an Analyst HT fluorescence plate reader. Each bar represents mean ± SD (error bars). n = 4 independent experiments. *$p < 0.05$, as determined by Student's t test.

(D) Schematic (top) of several cellular outcomes of NTERA-2-OP4k cells after the chemical screening. Representative fluorescent (center) and phase-contrast (bottom) images were taken from the actual screening and are shown for each outcome. Scale bar, 100 μm.

(E) Number of total compounds screened and hit compounds identified after each step of screening. The hit rates (in parentheses) were calculated based on the ratio of hit compounds and total compounds. Compounds from four different libraries (Marvel, NCI, house, and ChemBridge library) were screened. Because of the large number of compounds hosted by the libraries (171,077 compounds total), only one round of screening (n = 1) was performed for the entire compound collection.

See also Figure S1.

growth). A compound that fell into either of the two categories would have reduced the total number of cells in the treated well and, therefore, been able to lower its EGFP signal intensity without actually disrupting the pluripotent status of cells in that well. A real hit compound, however, would have downregulated EGFP expression on a cellular level (Figure 1D, Primary hits). To distinguish between the actual hit compounds and compounds that generated false positive signals, we inspected all wells that showed significant EGFP signal reduction under a fluorescence microscope immediately after the fluorescence plate reader scan. Based on the criteria described above and shown in Figure 1D, we identified the wells in which EGFP signals were reduced on a cellular level as true primary hits. As a result, although 2,865 compounds (1.7% of all compounds screened) were identified as candidate hits based on their reduced EGFP signals, only 214 of those compounds (0.13% of all compounds screened) were verified as primary hits (Figure 1E).

We then validated the pluripotency disruption activities of the primary hits in hESCs. Primary hit compounds were cherry-picked from the original screening plates and applied to hESCs at concentrations close to the concentrations used in the HTS (Supplemental Experimental Procedures). H1 and H9 hESCs were seeded as colonies and incubated with the compounds under the feeder-independent

pluripotency culture condition (Experimental Procedures) for 4–6 days. The medium was changed, and the compounds were replenished every day or every other day. Cultures were monitored every day for loss of compact colony morphologies as signs of differentiation. Compounds that failed to disrupt hESC colony integrity at the concentrations tested were examined again at 5- to 10-fold increased concentrations under the same condition. Finally, 122 compounds were found to disrupt hESC colony integrity (Figure 1E). These compounds are hereafter referred to as hESC-verified hits or verified hits.

From the verified hits, we selected the ones that showed strong potencies (effective at relatively low concentrations) at inducing hESC differentiation, acquired those compounds in bulk from commercial sources, and further verified their activities at the molecular level. Various techniques, including western blotting, qPCR, immunostaining, and FACS analysis, were used to examine changes in the expression of pluripotency markers upon treatment of those compounds. Of the more than 30 compounds tested in detail, 29 compounds efficiently downregulated the expression of pluripotency markers in H1 and H9 hESCs (data not shown).

The Compound Displurigen Potently Disrupts hESC Pluripotency

Of those 29 compounds, compound NSC375009 from the National Cancer Institute (NCI) library was one of the most potent. We hereafter refer to this compound as Displurigen (Displg for short) for its property as a "reagent that disrupts pluripotency" (Figure 2A). When applied at 5 μM for 6 days, the colony integrity of hESCs was completely disrupted, as evidenced by cells within the colonies spread out and migrated away from each other (Figure 2B). Protein levels of OCT4 and NANOG were also downregulated after 6 days of 5 μM Displg treatment, but SOX2 expression stayed roughly unchanged during this period (Figure S2A). FACS analysis under the same treatment condition also showed that, although the majority of cells lost OCT4 and NANOG expression on day 6, approximately 25% of the cells remained $OCT4^+NANOG^+$ (Figure S2B), indicating that roughly 25% of the population remained pluripotent even after 6 days of Displg treatment at 5 μM.

To achieve a more robust differentiation, we tested Displg at higher concentrations. We found that a 10 μM concentration was sufficient for Displg to nearly completely annihilate the $OCT4^+NANOG^+$ population (from 88.29% to 0.67%; Figure 2C) after only 4 days of treatment. Western blotting showed similar results at the protein level (Figure 2D). Both FACS analysis and western blotting results showed that protein levels of the pluripotency markers OCT4, NANOG, and SOX2 remained largely unchanged after 24 hr of 10 μM Displg treatment (Figures 2C and 2D). In contrast, qPCR results indicated that the mRNA levels of *OCT4* and *NANOG* decreased significantly after 24 hr of 10 μM Displg treatment and continued to decrease during the remaining course of differentiation (Figure 2E). These results showed that, upon Displg treatment, the changes of pluripotency marker expression at the mRNA level preceded those at the protein level, indicating that the primary regulatory pathway affected by Displg may be related to the regulation of mRNA. To rule out the possibility that Displg did not directly disrupt pluripotency but, rather, enriched differentiated or differentiating cells in the culture by selectively killing or inhibiting cell-cycle progression of pluripotent hESCs, we conducted apoptosis and cell-cycle analyses for 2-day and 4-day 10 μM Displg-treated cells. Apoptosis analysis using Annexin V and propidium iodide (PI) showed less than 5% apoptosis rates (Annexin V^+ populations) in samples treated with 10 μM Displg for 2 and 4 days, which were only mild elevations compared with DMSO controls (Figure S2C). Cell-cycle analysis using PI staining also showed that cell-cycle progression was not affected by 10 μM Displg treatment after 2 and 4 days. In fact, the percentages of G2/M phase cells even mildly increased in Displg-treated cells compared with DMSO controls (Figure S2D), possibly because of compensation effects against the increased cell deaths in Displg treatment samples (Figure S2C).

We then examined whether Displg induced epithelial-mesenchymal transition (EMT) and lineage-specific differentiation of hESCs. The epithelial marker E-cadherin and the mesenchymal markers N-cadherin and Fibronectin 1 (FN1) were examined in samples treated with 10 μM Displg for 1–4 days. E-cadherin mRNA expression was reduced significantly starting from day 2 and persisted through day 4, whereas N-cadherin and FN1 expression was consistently upregulated starting on day 2 and day 1, respectively (Figure 2F). To examine whether Displg induces lineage-specific differentiation, multiple lineage-specific marker genes (eight neuroectoderm markers, ten mesoderm markers, eight endoderm markers, and two trophectoderm markers) were selected and analyzed in H1 and H9 hESCs subjected to 6 days of differentiation under a basal differentiation medium (Supplemental Experimental Procedures) using qPCR. Three independent experiments were conducted. The overall average expression of each marker gene, presented as the relative level compared with DMSO control, was organized and is shown as heatmaps in Figure 2G (H1 hESC) and Figure S2E (H9 hESC). RA and HMBA were examined in parallel with Displg. Interestingly, although both RA and HMBA enhanced the expression of multiple lineage markers of various lineages, Displg inhibited the elevation of almost all differentiation markers examined, compared with DMSO controls, in both H1 and H9 hESCs (Figure 2G; Figure S2E). These data demonstrated that, apart from

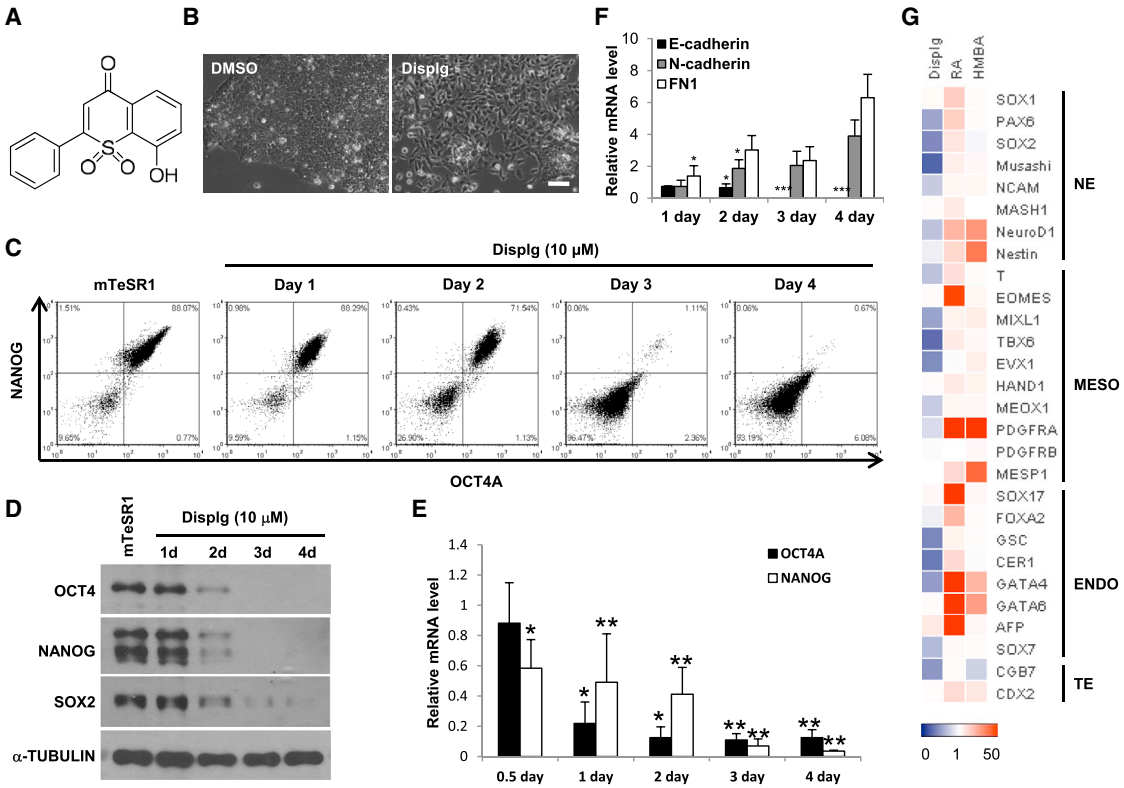

Figure 2. Compound NSC375009 (Displurigen) Disrupts hESC Pluripotency

(A) Chemical structure of compound NSC375009 (Displg).

(B) Phase-contrast images of H9 hESCs treated with DMSO and Displg (5 μM) for 2 days. Scale bar, 100 μm.

(C) Intracellular FACS analysis of OCT4A and NANOG in H1 hESCs left untreated (mTeSR1) or treated with 10 μM Displg for 1–4 days.

(D) Western blotting of OCT4, SOX2, and NANOG in H1 hESCs left untreated (mTeSR1) or treated with 10 μM Displg for 1–4 days (d). α-Tubulin was used as a loading control.

(E) qPCR analysis of *OCT4* and *NANOG* in H1 hESCs left untreated (mTeSR1) or treated with 10 μM Displg for 0.5–4 days. All values were normalized to the level (= 1) of mRNA in cells without compound treatment. Each bar represents mean ± SD (error bars). n = 3 independent experiments. *p < 0.05, **p < 0.01, as determined by Student's t test. *ACTB* (*β-actin*) was used as a loading control.

(F) qPCR analysis of epithelial (*E-cadherin*) and mesenchymal (*N-cadherin, FN1*) markers in H1 hESCs treated with 10 μM Displg for 1–4 days. All values were normalized to the level (= 1) of mRNA in cells without compound treatment. Each bar represents mean ± SD (error bars). n = 3 independent experiments. *p < 0.05, ***p < 0.001, as determined by Student's t test. *ACTB* (*β-actin*) was used as a loading control.

(G) Heatmap showing qPCR analysis of neuroectoderm (NE), mesoderm (MESO), endoderm (ENDO), and trophectoderm (TE) markers in H1 hESCs treated with Displg (10 μM), RA (10 μM), and HMBA (3 mM) for 6 days under differentiation conditions. All values were normalized to the level (= 1) of mRNA in the DMSO control. Each bar represents mean ± SD (error bars). The overall average value of relative mRNA expression from three independent experiments is shown. *ACTB* (*β-actin*) was used as a loading control.

See also Figure S2.

disrupting pluripotency, Displg also inhibited lineage-specific differentiation, indicating that the target of Displg may not only be required for maintaining pluripotency but also needed for supporting the proper lineage-selective differentiation of hESCs.

Displg Disrupts hESC Pluripotency by Targeting HSPA8

To identify the biological target of Displg, we synthesized a biotinylated version of the compound by linking a linker and a biotin molecule at the -OH site of Displg (Figure 3A). This molecule is hereafter referred to as Displg-biotin. Displg-biotin disrupted hESC pluripotency, as shown by loss of colony integrity and downregulation of OCT4 (Figures 3B and 3C), although at a higher dosage (50 μM) compared with unmodified Displg. This result indicates that Displg-biotin reserves the bioactivity of its parent compound Displg, although with a weaker potency. The decrease in potency of Displg-biotin may be due to the larger size of the molecule preventing its cellular uptake.

Using Displg-biotin as a probe, we conducted an affinity-based pull-down experiment (Experimental Procedures).

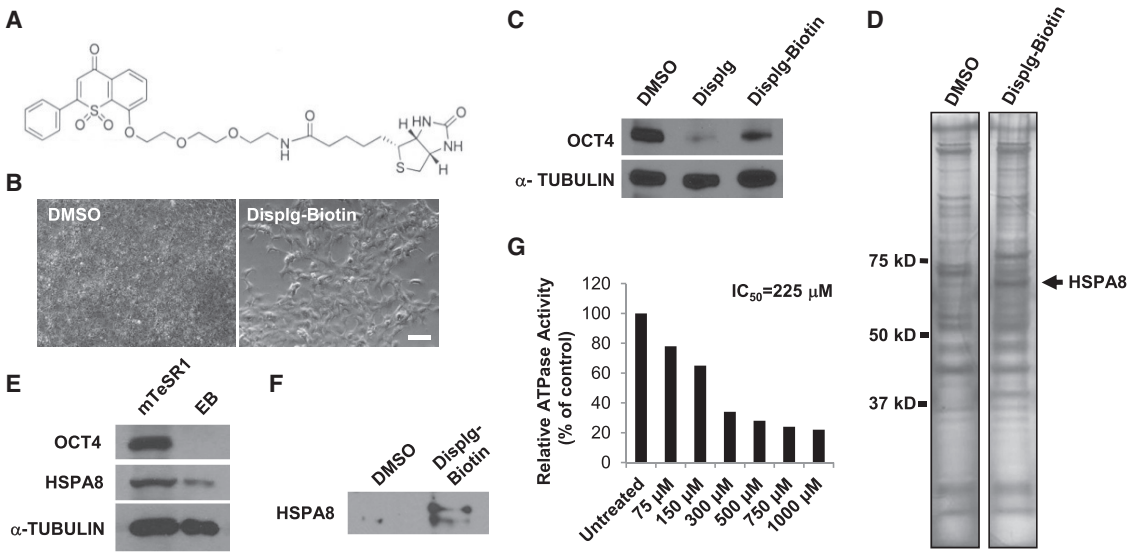

Figure 3. Displurigen Targets HSPA8

(A) Chemical structure of Displg-biotin.

(B) Phase-contrast images of H1 hESCs treated with DMSO and Displg-biotin (100 μM) for 4 days. Scale bar, 100 μm.

(C) Western blotting of OCT4 in H1 hESCs treated with DMSO, Displg (10 μM), and Displg-biotin (100 μM) for 6 days. α-Tubulin was used as a loading control.

(D) Silver staining of SDS-PAGE gel with proteins pulled down by Displg-biotin. DMSO was used as a control. Mass spectrometry analysis revealed HSPA8 protein as a target of Displg-biotin.

(E) Western blotting of OCT4 and HSPA8 isoform 1 in undifferentiated H1 hESCs versus H1 hESCs subjected to EB differentiation for 10 days. α-Tubulin was used as a loading control.

(F) Western blotting of HSPA8 isoform 1 in the precipitates of Displg-biotin (10 μM) and DMSO pull-down assays using H9 hESC lysates. Total lysates used were normalized between the DMSO and Displg-biotin pull-down assays.

(G) In vitro ATPase activity of HSP70 in the presence of increasing doses of Displurigen (n = 1 independent experiment).

See also Figure S3.

Briefly, hESCs treated with Displg-biotin or a DMSO control were lysed and then incubated with streptavidin beads. Proteins bound to Displg-biotin were eluted and analyzed using SDS-PAGE followed by silver staining. A distinct band was consistently observed in the Displg-biotin pull-down samples, but not in the control samples, at approximately 70 kDa and was identified to be HSPA8 (also known as HSC70) by mass spectrometry analysis with a score above the significance threshold ($p < 0.05$) (Figure 3D; Figure S3A). Three protein hits of human origin were identified in this analysis and are listed in Figure S3A. Two keratin proteins were identified but excluded from being considered as potential hits because keratins are known to be common contaminants of mass spectrometry (Lavallée-Adam et al., 2011). Seven unique trypsin-digested peptide fragments were identified for HSPA8, Their respective positions within the protein sequence are shown in Figure S3B.

HSPA8 is the constitutively expressed member of the 70-kDa heat shock protein family, as opposed to the stress-induced HSP70. Two previous publications (Fathi et al., 2009; Son et al., 2005) show that HSPA8 is expressed in undifferentiated hESCs but downregulated upon differentiation. In our hands, however, 4 days of Displg treatment at 10 μM were not enough to downregulate HSPA8 expression at the protein level (Figure S3C). We argue that, as a constitutively expressed heat shock protein that is vital to the routine functioning of the cells, the expression of HSPA8 may have been maintained by multiple pathways simultaneously and may not be easily downregulated within 4 days of differentiation. Indeed, our data showed that HSPA8 was dramatically downregulated after 10 days of embryoid body (EB) differentiation (Figure 3E; Supplemental Experimental Procedures), revealing a link between HSPA8 expression and hESC pluripotency. We therefore hypothesized that HSPA8 may be the biological target of Displg.

To test this hypothesis, we first confirmed the interaction between Displg and HSPA8 by applying the pull-down samples to western blotting, which showed that Displg indeed bound to and pulled down HSPA8 (Figure 3F). We also performed an in vitro ATPase assay using recombinant HSP70, which is structurally highly similar to

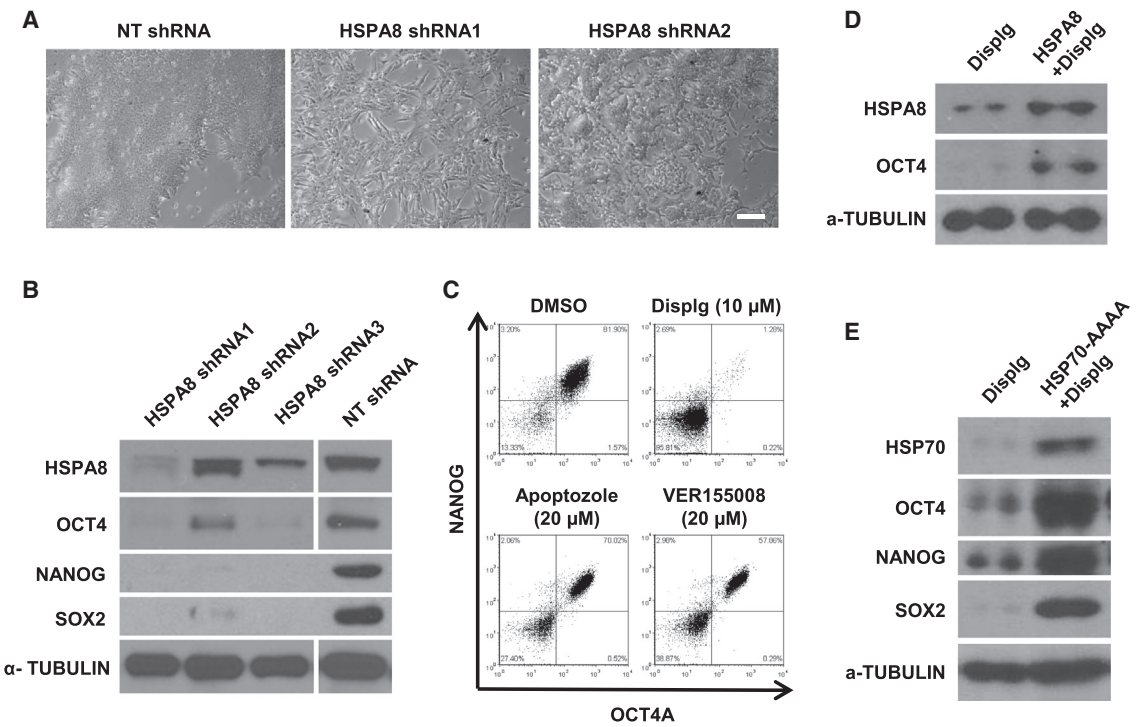

Figure 4. HSPA8 is the Biological Target of Displurigen.

(A) Phase-contrast images of H9 hESCs infected with lentivirus particles containing non-target (NT) shRNA or shRNAs (shRNA1 and shRNA2; Supplemental Experimental Procedures) targeting HSPA8 isoform 1 for 5 days. Scale bar, 100 μm.

(B) Western blotting of HSPA8 isoform 1, OCT4, SOX2, and NANOG in H1 hESCs infected with lentivirus particles containing NT shRNA and HSPA8-1-targeting shRNAs. A lane showing OCT4 shRNA knockdown (KD) as a positive control was cropped (shown as gaps) from the HSPA8, OCT4, and α-tubulin strips. The uncropped image is shown in Figure S4. α-Tubulin was used as a loading control.

(C) Intracellular FACS analysis of OCT4A and NANOG in H1 hESCs treated with DMSO, 10 μM Displurigen, 20 μM Apoptozole, and 20 μM VER155008 for 4 days.

(D) Western blotting of HSPA8 isoform 1 and OCT4 in H1 hESCs treated with 10 μM Displg for 6 days with or without HSPA8 overexpression. α-Tubulin was used as a loading control.

(E) Western blotting of HSP70, OCT4, SOX2, and NANOG in H9 hESCs treated with 5 μM Displg for 16 days with or without overexpression of HSP70-AAAA. α-Tubulin was used as a loading control.

See also Figure S4.

HSPA8 (Stricher et al., 2013), and showed that Displg inhibited the ATPase activity of HSP70 with a half-maximal inhibitory concentration (IC_{50}) of 225 μM (Figure 3G). We then conducted loss-of-function experiments to examine whether HSPA8 was the true biological target of Displg in regard to its activity in disrupting pluripotency. Knockdown of HSPA8 in hESCs using short hairpin RNAs (shRNAs) disrupted pluripotency, as shown by loss of colony integrity (Figure 4A) and downregulation of the pluripotency markers OCT4, NANOG, and SOX2 (Figure 4B; Figure S4 shows the uncropped blot). Other commercially available HSP70/HSPA8 inhibitors, including Apoptozole (Cho et al., 2011) (20 μM) and VER155008 (Massey et al., 2010) (20 μM) also disrupted hESC pluripotency, although less potently compared with Displg (Figure 4C). These results demonstrate that HSPA8 is likely to be the biological target of Displg responsible for maintaining hESC pluripotency.

To further verify HSPA8 as the primary target of Displg in pluripotency maintenance, we attempted to rescue the pluripotency disruption effect of Displg by overexpressing HSPA8 in hESCs. We first overexpressed wild-type HSPA8 protein, which rescued the effect of Displg, as shown by the elevated OCT4 expression (Figure 4D). The efficiency of this rescue was modest, which may be attributed to the fact that overexpression of wild-type chaperone proteins has been known to be harmful to cells (Freeman et al., 1995). To achieve a more robust rescue, we overexpressed a chaperone-dead mutant form of HSP70 protein, named HSP70-AAAA (Freeman et al., 1995), in which the last four amino acids were mutated from EEVD to AAAA. Indeed, overexpression of HSP70-AAAA gave rise to a

more robust rescue of Displg, as demonstrated by the pluripotency marker expressions (Figure 4E). These results confirmed HSPA8 as the biological target of Displg and further verified the function of HSPA8 in pluripotency maintenance.

HSPA8 Maintains Pluripotency by Facilitating the DNA-Binding Activity of OCT4

Heat shock proteins, as molecular chaperones, are involved in a variety of cellular processes, including maintenance of protein stability (Wegele et al., 2004), mediating the assembly and disassembly of protein complexes (Ellis, 2007), and the more recently discovered role of regulating the dynamics of protein-DNA association events such as transcription (Freeman and Yamamoto, 2002; Müller et al., 2004; Shaknovich et al., 1992; Stavreva et al., 2004; Walerych et al., 2004). Our data showed that the downregulation of core pluripotency factors at the mRNA level preceded the downregulation of those factors at the protein level (Figures 2C–2E). Specifically, mRNA levels of the pluripotency factors were downregulated within the first 24 hr of Displg treatment (Figure 2E), whereas their protein levels remained largely unchanged after 24 hr of treatment (Figures 2C and 2D). This distinct dynamic indicated that HSPA8 most likely regulated the core pluripotency network at the mRNA level. We therefore focused our efforts on investigating the role of HSPA8 in regulating the transcription of the core pluripotency factors.

As discussed in the Introduction, the core pluripotency regulators OCT4, NANOG, and SOX2 form a core transcription regulatory network through auto- and reciprocal activations at the transcription level. This core network is supported by an expanded network composed of a large number of protein factors belonging to distinct functional categories. We hypothesized that HSPA8 belongs to this expanded network of protein factors and maintains pluripotency through interacting with the core pluripotency factors and facilitating their transcription-activation activities (Freeman and Yamamoto, 2002; Müller et al., 2004; Shaknovich et al., 1992; Stavreva et al., 2004; Walerych et al., 2004). A nuclear fractionation assay demonstrated that HSPA8 proteins are indeed present in the nuclei of undifferentiated hESCs (Figure S5A), confirming the validity of our hypothesis. For simplicity, we focused our study on examining the interaction between HSPA8 and the master pluripotency regulator OCT4. Indeed, co-immunoprecipitation (coIP) experiments showed that HSPA8 bound to OCT4 and that this interaction was disrupted by Displg (Figure 5A).

To test our hypothesis, we examined whether HSPA8 was required for OCT4 protein to efficiently bind to DNA. We first tested this potential regulatory mechanism using electrophoretic mobility shift assay (EMSA) and discovered that Displg effectively reduced the binding affinities of OCT4 to its DNA-binding motifs located in the *OCT4*, *NANOG*, and *SOX2* promoters (Catena et al., 2004; Chew et al., 2005; Rodda et al., 2005; Figure 5B). Two distinct bands (A and B; Figure 5B) were detected in EMSA. A supershift assay using anti-OCT4 antibody was conducted that showed band A as the band representing OCT4 binding to the DNA probes (Figure S5B). Three independent experiments demonstrated that this inhibitory effect of Displg was consistent and robust (Figure 5C) and indicated that the activity of HSPA8 was necessary for OCT4 protein to efficiently bind to DNA. We then examined whether this regulatory effect depends on the presence of other protein factors by conducting an in vitro binding assay using recombinant OCT4 and HSP70 proteins. OCT4 alone only exhibited a weak binding affinity to DNA, whereas the addition of 1–10 μM recombinant HSP70 dramatically enhanced the OCT4-DNA interaction (Figure 5D). Without OCT4, 10 μM HSP70 alone did not exhibit any detectable DNA binding activity (Figure S5C; Figure S5D shows the uncropped blot). Notably, 1 μM HSP70 protein was sufficient to efficiently boost the DNA binding activity of OCT4 from 100% in the OCT4-only control to an average of 213% ± 26% ($p < 0.01$), based on the quantification of band intensities from three independent experiments using ImageJ. Because the combined cellular concentration of the constitutively expressed and stress-induced forms of 70-kDa heat shock proteins under normal physiological conditions is approximately 24 μM (Ghaemmaghami et al., 2003; Jorgensen et al., 2007), the 1-μM concentration of HSP70 tested in this experiment is well within its physiological range and should not cause unwanted experimental artifacts. This result suggests that HSPA8 facilitates the association of OCT4-DNA complexes in a direct fashion independent of other protein factors.

DISCUSSION

In this study, we established an NTERA-2 hECC-based pluripotency reporter system and screened 171,077 compounds. We identified 29 bioactive small molecules that potently disrupted hESC pluripotency, as evidenced by changes in pluripotency marker expressions, and studied one particular molecule, Displurigen, in detail. Using target identification techniques and functional verifications, we discovered HSPA8 as the biological target of Displurigen.

HTS has been used for the discovery of novel small molecule compounds that regulate PSC fate. Such studies require the use of pluripotent cell lines as screening platforms. Commonly available pluripotent platforms include mouse and human ESCs, mouse and human ECCs, and the more recently established mouse and human iPSCs. The

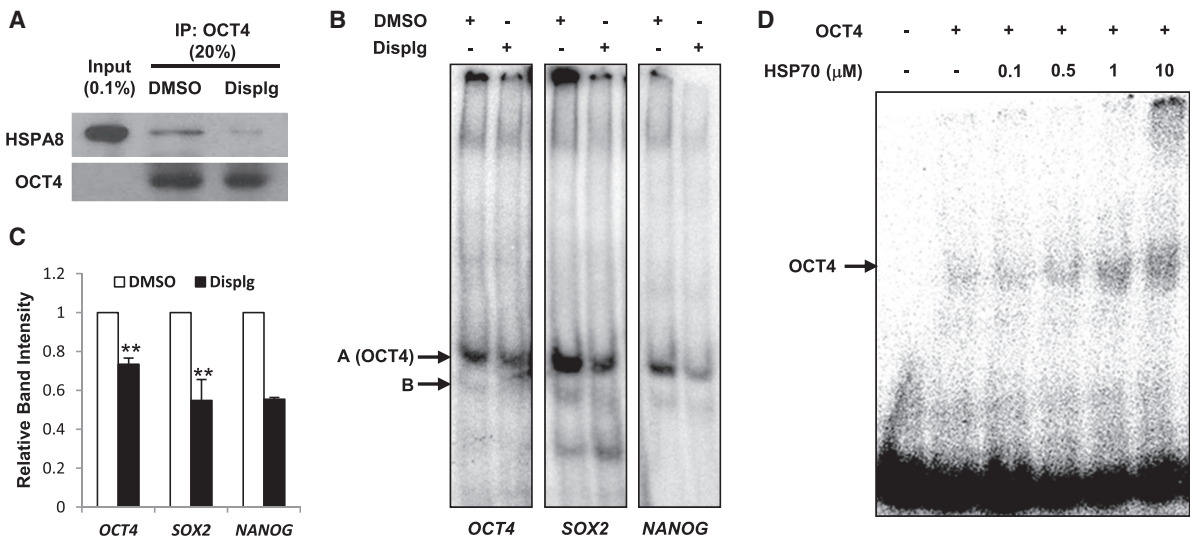

Figure 5. HSPA8 Regulates the DNA-Binding Activity of OCT4

(A) Immunoprecipitation (IP) of OCT4 from H1 hESC lysates treated with DMSO or Displg (1 mM), followed by western blotting of OCT4 and HSPA8 isoform 1.

(B) EMSA using labeled OCT4-binding elements from the *OCT4*, *SOX2*, and *NANOG* promoters to detect bindings of protein factors in the nuclear extracts of H9 hESCs with or without Displurigen treatment (10 μM, 24 hr). A and B denote potential DNA-protein complexes, with band A being the band representing OCT4-binding to the DNA probes (see also Figure S5B).

(C) Quantification of relative band intensities from three independent EMSA experiments using ImageJ. All values were normalized to the level (= 1) of band intensity in the DMSO control. Each bar represents mean ± SD (error bars). $^{**}p < 0.01$, as determined by Student's t test.

(D) EMSA showing binding (arrow) of purified recombinant OCT4 proteins (500 ng/reaction) to a labeled OCT4-binding element in vitro with or without the addition of purified recombinant HSP70 proteins (up to 10 μM).

See also Figure S5.

earliest attempts of pluripotency regulator screenings adopted mouse embryonic stem cells (mESCs) and mouse embryonal carcinoma cells (mECCs) as their screening platforms (Chen et al., 2006; Ding et al., 2003; Zhu et al., 2009). More recently, several hESC- and hiPSC-based HTSs have been reported (Barbaric et al., 2010; Ben-David et al., 2013; Desbordes et al., 2008; Gonzalez et al., 2011b; Kameoka et al., 2014; Kumagai et al., 2013; Manganelli et al., 2014; Xu et al., 2010). Compared with those platforms, we believe that hECCs have been underappreciated for HTS. hECCs are cheap and easy to passage and maintain, are robust in maintaining a pluripotent state and not prone to spontaneous differentiation, and are of human origin and highly similar to hESCs in their molecular regulatory mechanism of pluripotency (Josephson et al., 2007). These qualities collectively make hECCs an ideal system for HTS purposes, but, to date, to our knowledge, only one attempt has been made to use hECCs for a HTS study in which 80 chemical compounds were screened (Barbaric et al., 2011). In comparison, our hECC-based HTS platform was used to successfully screen a significant number (171,077) of chemical compounds in this study.

Heat shock proteins, as molecular chaperones, are involved in a variety of cellular functions. Apart from their commonly known roles in maintaining protein stability and mediating the assembly and disassembly of protein complexes, recent studies have shown that certain chaperones, including HSPA8, also regulate the dynamic formation of protein-DNA complexes involved in biological processes such as transcription, telomere maintenance, DNA repair, and DNA replication (Ahn et al., 2005; DeZwaan and Freeman, 2010). Although a previous report has demonstrated a regulatory role of the chaperone protein Hsp90 in maintaining mESC pluripotency through interacting with the core pluripotency factors (Bradley et al., 2012), the possible role of chaperones in directly regulating the DNA-binding and, subsequently, the transcription-activation activities of the core pluripotency factors has yet to be investigated. Our study examined this potential molecular mechanism and unveiled a function of the chaperone protein HSPA8 in maintaining hESC pluripotency by directly facilitating the transcription-activation activity of the master pluripotency factor OCT4.

Our study also adds another HSPA8/HSP70 inhibitor, Displurigen, to the current reservoir of bioactive small molecules. The modulation of heat shock protein activities has been studied extensively for potential clinical applications such as cancer therapy. In contrast to normal cells, cancer

cells strongly overexpress HSP70 to provide resistance to stresses generated by the environment, from tumorigenesis events, and during cancer therapy. This addiction to HSP70 provides the theoretical basis for its targeting in anti-cancer treatment (Goloudina et al., 2012; Jego et al., 2013). In recent years, several HSPA8/HSP70 inhibitors have been discovered and studied for their applications in anti-cancer therapies (Goloudina et al., 2012). The discovery of Displurigen expands this growing list of HSPA8/HSP70 inhibitors and provides a drug candidate for cancer therapy.

In summary, by establishing and applying a hECC-based HTS system, our study identifies a chemical inhibitor of HSPA8/HSP70 and unveils a chaperone-related molecular mechanism for the maintenance of hESC pluripotency.

EXPERIMENTAL PROCEDURES

Generation and Validation of NTERA-2-OP4k Reporter Cells

The plasmid containing EGFP driven by a fragment of the OCT4 promoter (~4 kb) was provided by Dr. Wei Cui (Imperial College London) and was as described previously (Gerrard et al., 2005). NTERA-2-OP4k cells were established and validated as described in the Supplemental Experimental Procedures.

Large-Scale Chemical Screening

Large-scale chemical screening was conducted at the High-Throughput Screening Facility (HTSF) at the University of Illinois at Urbana-Champaign (http://www.scs.illinois.edu/htsf/index.html). The HTSF hosts 171,077 compounds from several compound libraries, including the Marvel Library, the HTSF house library, the ChemBridge MicroFormat library, and the NCI library. Because of the large number of compounds hosted by the libraries, only one round of screening (n = 1) was performed for the entire compound collection. Detailed procedures of this screen are described in the Supplemental Experimental Procedures.

Affinity Chromatography, Electrophoresis, and Silver Staining

hESCs were cultured under the feeder-independent condition with or without the presence of displurigen-biotin (10 μM) overnight. Cells were collected and subjected to affinity chromatography, electrophoresis, and silver staining as described in the Supplemental Experimental Procedures.

SUPPLEMENTAL INFORMATION

Supplemental Information includes Supplemental Experimental Procedures, five figures, and four tables and can be found with this article online at http://dx.doi.org/10.1016/j.stemcr.2015.09.023.

AUTHOR CONTRIBUTIONS

Y.G., Y.Z., and L.C.S. conceived and designed the experiments. Y.Z. synthesized and purified Displurigen-biotin. Y.G., L.C.S., B.F., D.A.L., K.M.A., J.D.S., and J.D.M. performed the experiments. Y.G., L.C.S., and B.F. analyzed the data. Y.G. wrote the manuscript.

ACKNOWLEDGMENTS

We thank Dr. Wei Cui for providing the OCT4-EGFP reporter construct, Dr. Karson Putt for technical assistance with HTS, Dr. Peter Yau for technical assistance with LC-MS, and Dr. Brian Freeman and Dr. Jianjun Cheng for valuable scientific discussions. This work was supported by the NIH (GM083812), the Illinois Regenerative Medicine Institute (IDPH 2006-05516), a National Science Foundation (NSF) CAREER award (0953267), and NSF Science and Technology Center Emergent Behaviors of Integrated Cellular Systems (EBICS) (CBET-0939511).

Received: March 20, 2015
Revised: September 28, 2015
Accepted: September 29, 2015
Published: November 5, 2015

REFERENCES

Ahn, S.G., Kim, S.A., Yoon, J.H., and Vacratsis, P. (2005). Heat-shock cognate 70 is required for the activation of heat-shock factor 1 in mammalian cells. Biochem. J. *392*, 145–152.

Andrews, P.W. (1984). Retinoic acid induces neuronal differentiation of a cloned human embryonal carcinoma cell line in vitro. Dev. Biol. *103*, 285–293.

Andrews, P.W., Damjanov, I., Simon, D., Banting, G.S., Carlin, C., Dracopoli, N.C., and Føgh, J. (1984). Pluripotent embryonal carcinoma clones derived from the human teratocarcinoma cell line Tera-2. Differentiation in vivo and in vitro. Lab. Invest. *50*, 147–162.

Andrews, P.W., Gönczöl, E., Plotkin, S.A., Dignazio, M., and Oosterhuis, J.W. (1986). Differentiation of TERA-2 human embryonal carcinoma cells into neurons and HCMV permissive cells. Induction by agents other than retinoic acid. Differentiation *31*, 119–126.

Andrews, P.W., Nudelman, E., Hakomori, S., and Fenderson, B.A. (1990). Different patterns of glycolipid antigens are expressed following differentiation of TERA-2 human embryonal carcinoma cells induced by retinoic acid, hexamethylene bisacetamide (HMBA) or bromodeoxyuridine (BUdR). Differentiation *43*, 131–138.

Andrews, P.W., Damjanov, I., Berends, J., Kumpf, S., Zappavigna, V., Mavilio, F., and Sampath, K. (1994). Inhibition of proliferation and induction of differentiation of pluripotent human embryonal carcinoma cells by osteogenic protein-1 (or bone morphogenetic protein-7). Lab. Invest. *71*, 243–251.

Barbaric, I., Gokhale, P.J., Jones, M., Glen, A., Baker, D., and Andrews, P.W. (2010). Novel regulators of stem cell fates identified by a multivariate phenotype screen of small compounds on human embryonic stem cell colonies. Stem Cell Res. (Amst.) *5*, 104–119.

Barbaric, I., Jones, M., Harley, D.J., Gokhale, P.J., and Andrews, P.W. (2011). High-content screening for chemical modulators of embryonal carcinoma cell differentiation and survival. J. Biomol. Screen. *16*, 603–617.

Ben-David, U., Gan, Q.F., Golan-Lev, T., Arora, P., Yanuka, O., Oren, Y.S., Leikin-Frenkel, A., Graf, M., Garippa, R., Boehringer, M., et al. (2013). Selective elimination of human pluripotent stem cells by an oleate synthesis inhibitor discovered in a high-throughput screen. Cell Stem Cell *12*, 167–179.

Borowiak, M., Maehr, R., Chen, S., Chen, A.E., Tang, W., Fox, J.L., Schreiber, S.L., and Melton, D.A. (2009). Small molecules efficiently direct endodermal differentiation of mouse and human embryonic stem cells. Cell Stem Cell *4*, 348–358.

Boyer, L.A., Lee, T.I., Cole, M.F., Johnstone, S.E., Levine, S.S., Zucker, J.P., Guenther, M.G., Kumar, R.M., Murray, H.L., Jenner, R.G., et al. (2005). Core transcriptional regulatory circuitry in human embryonic stem cells. Cell *122*, 947–956.

Bradley, E., Bieberich, E., Mivechi, N.F., Tangpisuthipongsa, D., and Wang, G. (2012). Regulation of embryonic stem cell pluripotency by heat shock protein 90. Stem Cells *30*, 1624–1633.

Catena, R., Tiveron, C., Ronchi, A., Porta, S., Ferri, A., Tatangelo, L., Cavallaro, M., Favaro, R., Ottolenghi, S., Reinbold, R., et al. (2004). Conserved POU binding DNA sites in the Sox2 upstream enhancer regulate gene expression in embryonic and neural stem cells. J. Biol. Chem. *279*, 41846–41857.

Chen, S., Do, J.T., Zhang, Q., Yao, S., Yan, F., Peters, E.C., Schöler, H.R., Schultz, P.G., and Ding, S. (2006). Self-renewal of embryonic stem cells by a small molecule. Proc. Natl. Acad. Sci. USA *103*, 17266–17271.

Chen, S., Borowiak, M., Fox, J.L., Maehr, R., Osafune, K., Davidow, L., Lam, K., Peng, L.F., Schreiber, S.L., Rubin, L.L., and Melton, D. (2009). A small molecule that directs differentiation of human ESCs into the pancreatic lineage. Nat. Chem. Biol. *5*, 258–265.

Chen, Y.S., Pelekanos, R.A., Ellis, R.L., Horne, R., Wolvetang, E.J., and Fisk, N.M. (2012). Small molecule mesengenic induction of human induced pluripotent stem cells to generate mesenchymal stem/stromal cells. Stem Cells Transl. Med. *1*, 83–95.

Chew, J.L., Loh, Y.H., Zhang, W., Chen, X., Tam, W.L., Yeap, L.S., Li, P., Ang, Y.S., Lim, B., Robson, P., and Ng, H.H. (2005). Reciprocal transcriptional regulation of Pou5f1 and Sox2 via the Oct4/Sox2 complex in embryonic stem cells. Mol. Cell. Biol. *25*, 6031–6046.

Cho, H.J., Gee, H.Y., Baek, K.H., Ko, S.K., Park, J.M., Lee, H., Kim, N.D., Lee, M.G., and Shin, I. (2011). A small molecule that binds to an ATPase domain of Hsc70 promotes membrane trafficking of mutant cystic fibrosis transmembrane conductance regulator. J. Am. Chem. Soc. *133*, 20267–20276.

Desbordes, S.C., Placantonakis, D.G., Ciro, A., Socci, N.D., Lee, G., Djaballah, H., and Studer, L. (2008). High-throughput screening assay for the identification of compounds regulating self-renewal and differentiation in human embryonic stem cells. Cell Stem Cell *2*, 602–612.

DeZwaan, D.C., and Freeman, B.C. (2010). HSP90 manages the ends. Trends Biochem. Sci. *35*, 384–391.

Ding, S., Wu, T.Y.H., Brinker, A., Peters, E.C., Hur, W., Gray, N.S., and Schultz, P.G. (2003). Synthetic small molecules that control stem cell fate. Proc. Natl. Acad. Sci. USA *100*, 7632–7637.

Draper, J.S., Pigott, C., Thomson, J.A., and Andrews, P.W. (2002). Surface antigens of human embryonic stem cells: changes upon differentiation in culture. J. Anat. *200*, 249–258.

Ellis, R.J. (2007). Protein misassembly: macromolecular crowding and molecular chaperones. Adv. Exp. Med. Biol. *594*, 1–13.

Fathi, A., Pakzad, M., Taei, A., Brink, T.C., Pirhaji, L., Ruiz, G., Sharif Tabe Bordbar, M., Gourabi, H., Adjaye, J., Baharvand, H., and Salekdeh, G.H. (2009). Comparative proteome and transcriptome analyses of embryonic stem cells during embryoid body-based differentiation. Proteomics *9*, 4859–4870.

Freeman, B.C., and Yamamoto, K.R. (2002). Disassembly of transcriptional regulatory complexes by molecular chaperones. Science *296*, 2232–2235.

Freeman, B.C., Myers, M.P., Schumacher, R., and Morimoto, R.I. (1995). Identification of a regulatory motif in Hsp70 that affects ATPase activity, substrate binding and interaction with HDJ-1. EMBO J. *14*, 2281–2292.

Gerrard, L., Zhao, D., Clark, A.J., and Cui, W. (2005). Stably transfected human embryonic stem cell clones express OCT4-specific green fluorescent protein and maintain self-renewal and pluripotency. Stem Cells *23*, 124–133.

Ghaemmaghami, S., Huh, W.K., Bower, K., Howson, R.W., Belle, A., Dephoure, N., O'Shea, E.K., and Weissman, J.S. (2003). Global analysis of protein expression in yeast. Nature *425*, 737–741.

Goloudina, A.R., Demidov, O.N., and Garrido, C. (2012). Inhibition of HSP70: a challenging anti-cancer strategy. Cancer Lett. *325*, 117–124.

Gonzalez, R., Lee, J.W., and Schultz, P.G. (2011a). Stepwise chemically induced cardiomyocyte specification of human embryonic stem cells. Angew. Chem. Int. Ed. Engl. *50*, 11181–11185.

Gonzalez, R., Lee, J.W., Snyder, E.Y., and Schultz, P.G. (2011b). Dorsomorphin promotes human embryonic stem cell self-renewal. Angew. Chem. Int. Ed. Engl. *50*, 3439–3441.

Jego, G., Hazoumé, A., Seigneuric, R., and Garrido, C. (2013). Targeting heat shock proteins in cancer. Cancer Lett. *332*, 275–285.

Jorgensen, P., Edgington, N.P., Schneider, B.L., Rupes, I., Tyers, M., and Futcher, B. (2007). The size of the nucleus increases as yeast cells grow. Mol. Biol. Cell *18*, 3523–3532.

Josephson, R., Ording, C.J., Liu, Y., Shin, S., Lakshmipathy, U., Toumadje, A., Love, B., Chesnut, J.D., Andrews, P.W., Rao, M.S., and Auerbach, J.M. (2007). Qualification of embryonal carcinoma 2102Ep as a reference for human embryonic stem cell research. Stem Cells *25*, 437–446.

Kameoka, S., Babiarz, J., Kolaja, K., and Chiao, E. (2014). A high-throughput screen for teratogens using human pluripotent stem cells. Toxicol. Sci. *137*, 76–90.

Kumagai, H., Suemori, H., Uesugi, M., Nakatsuji, N., and Kawase, E. (2013). Identification of small molecules that promote human embryonic stem cell self-renewal. Biochem. Biophys. Res. Commun. *434*, 710–716.

Lavallée-Adam, M., Cloutier, P., Coulombe, B., and Blanchette, M. (2011). Modeling contaminants in AP-MS/MS experiments. J. Proteome Res. *10*, 886–895.

Lian, X., Hsiao, C., Wilson, G., Zhu, K., Hazeltine, L.B., Azarin, S.M., Raval, K.K., Zhang, J., Kamp, T.J., and Palecek, S.P. (2012). Robust cardiomyocyte differentiation from human pluripotent stem cells via temporal modulation of canonical Wnt signaling. Proc. Natl. Acad. Sci. USA *109*, E1848–E1857.

Mahmood, A., Harkness, L., Schrøder, H.D., Abdallah, B.M., and Kassem, M. (2010). Enhanced differentiation of human embryonic stem cells to mesenchymal progenitors by inhibition of TGF-beta/activin/nodal signaling using SB-431542. J. Bone Miner. Res. *25*, 1216–1233.

Manganelli, G., Masullo, U., and Filosa, S. (2014). HTS/HCS to screen molecules able to maintain embryonic stem cell self-renewal or to induce differentiation: overview of protocols. Stem Cell Rev. *10*, 802–819.

Massey, A.J., Williamson, D.S., Browne, H., Murray, J.B., Dokurno, P., Shaw, T., Macias, A.T., Daniels, Z., Geoffroy, S., Dopson, M., et al. (2010). A novel, small molecule inhibitor of Hsc70/Hsp70 potentiates Hsp90 inhibitor induced apoptosis in HCT116 colon carcinoma cells. Cancer Chemother. Pharmacol. *66*, 535–545.

Müller, L., Schaupp, A., Walerych, D., Wegele, H., and Buchner, J. (2004). Hsp90 regulates the activity of wild type p53 under physiological and elevated temperatures. J. Biol. Chem. *279*, 48846–48854.

Rodda, D.J., Chew, J.L., Lim, L.H., Loh, Y.H., Wang, B., Ng, H.H., and Robson, P. (2005). Transcriptional regulation of nanog by OCT4 and SOX2. J. Biol. Chem. *280*, 24731–24737.

Shaknovich, R., Shue, G., and Kohtz, D.S. (1992). Conformational activation of a basic helix-loop-helix protein (MyoD1) by the C-terminal region of murine HSP90 (HSP84). Mol. Cell. Biol. *12*, 5059–5068.

Son, Y.S., Park, J.H., Kang, Y.K., Park, J.S., Choi, H.S., Lim, J.Y., Lee, J.E., Lee, J.B., Ko, M.S., Kim, Y.S., et al. (2005). Heat shock 70-kDa protein 8 isoform 1 is expressed on the surface of human embryonic stem cells and downregulated upon differentiation. Stem Cells *23*, 1502–1513.

Stavreva, D.A., Müller, W.G., Hager, G.L., Smith, C.L., and McNally, J.G. (2004). Rapid glucocorticoid receptor exchange at a promoter is coupled to transcription and regulated by chaperones and proteasomes. Mol. Cell. Biol. *24*, 2682–2697.

Stricher, F., Macri, C., Ruff, M., and Muller, S. (2013). HSPA8/HSC70 chaperone protein: structure, function, and chemical targeting. Autophagy *9*, 1937–1954.

Thomson, J.A., Itskovitz-Eldor, J., Shapiro, S.S., Waknitz, M.A., Swiergiel, J.J., Marshall, V.S., and Jones, J.M. (1998). Embryonic stem cell lines derived from human blastocysts. Science *282*, 1145–1147.

Walerych, D., Kudla, G., Gutkowska, M., Wawrzynow, B., Muller, L., King, F.W., Helwak, A., Boros, J., Zylicz, A., and Zylicz, M. (2004). Hsp90 chaperones wild-type p53 tumor suppressor protein. J. Biol. Chem. *279*, 48836–48845.

Watanabe, K., Ueno, M., Kamiya, D., Nishiyama, A., Matsumura, M., Wataya, T., Takahashi, J.B., Nishikawa, S., Nishikawa, S., Muguruma, K., and Sasai, Y. (2007). A ROCK inhibitor permits survival of dissociated human embryonic stem cells. Nat. Biotechnol. *25*, 681–686.

Wegele, H., Müller, L., and Buchner, J. (2004). Hsp70 and Hsp90–a relay team for protein folding. Rev. Physiol. Biochem. Pharmacol. *151*, 1–44.

Xu, R.H., Chen, X., Li, D.S., Li, R., Addicks, G.C., Glennon, C., Zwaka, T.P., and Thomson, J.A. (2002). BMP4 initiates human embryonic stem cell differentiation to trophoblast. Nat. Biotechnol. *20*, 1261–1264.

Xu, Y., Shi, Y., and Ding, S. (2008). A chemical approach to stem-cell biology and regenerative medicine. Nature *453*, 338–344.

Xu, Y., Zhu, X., Hahm, H.S., Wei, W., Hao, E., Hayek, A., and Ding, S. (2010). Revealing a core signaling regulatory mechanism for pluripotent stem cell survival and self-renewal by small molecules. Proc. Natl. Acad. Sci. USA *107*, 8129–8134.

Zhu, S., Wurdak, H., Wang, J., Lyssiotis, C.A., Peters, E.C., Cho, C.Y., Wu, X., and Schultz, P.G. (2009). A small molecule primes embryonic stem cells for differentiation. Cell Stem Cell *4*, 416–426.

zur Nieden, N.I., Kempka, G., Rancourt, D.E., and Ahr, H.J. (2005). Induction of chondro-, osteo- and adipogenesis in embryonic stem cells by bone morphogenetic protein-2: effect of cofactors on differentiating lineages. BMC Dev. Biol. *5*, 1.

Stem Cell Reports, Volume *5*

Supplemental Information

A Chemical Biology Study of Human Pluripotent Stem Cells Unveils HSPA8 as a Key Regulator of Pluripotency

Yijie Geng, Yongfeng Zhao, Lisa Corinna Schuster, Bradley Feng, Dana A. Lynn, Katherine M. Austin, Jason Daniel Stoklosa, and Joseph D. Morrison

SUPPLEMENTAL DATA

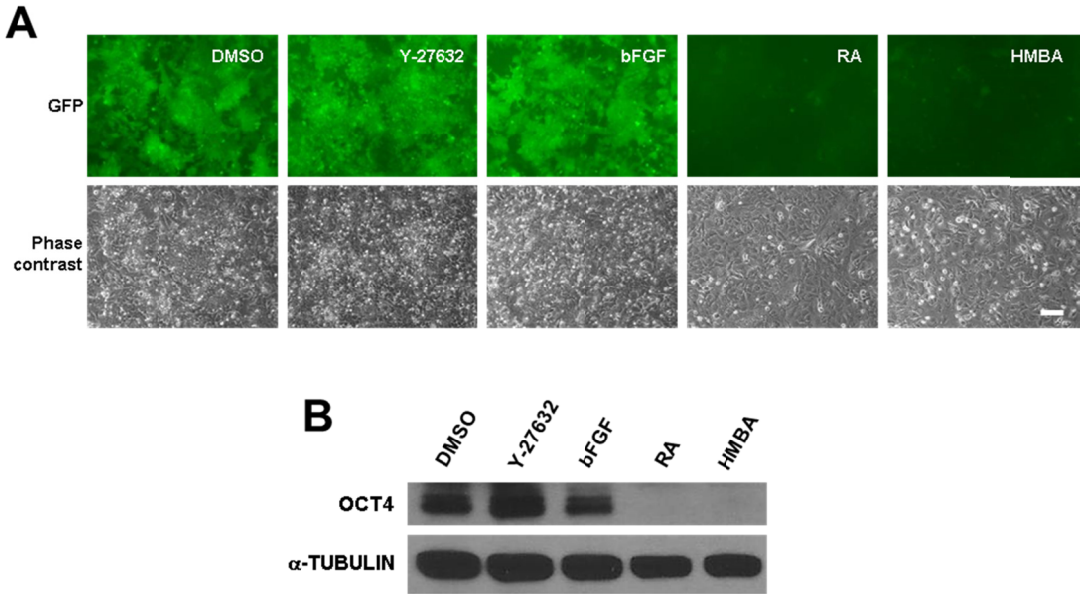

Figure S1, related to Figure 1. (**A**) Fluorescent (top panel) and phase contrast (bottom panel) images of NTERA-2-OP4k cells treated with DMSO, Y-27632 (10 μM), bFGF (4 ng/ml), retinoic acid (RA; 10 μM) and HMBA (3 mM) for 6 days. Scale bar: 100 μm. (**B**) Western blotting of OCT4 in NTERA-2-OP4k cells treated with DMSO, Y-27632, bFGF, RA, and HMBA for 7 days. α-TUBULIN was used as a loading control.

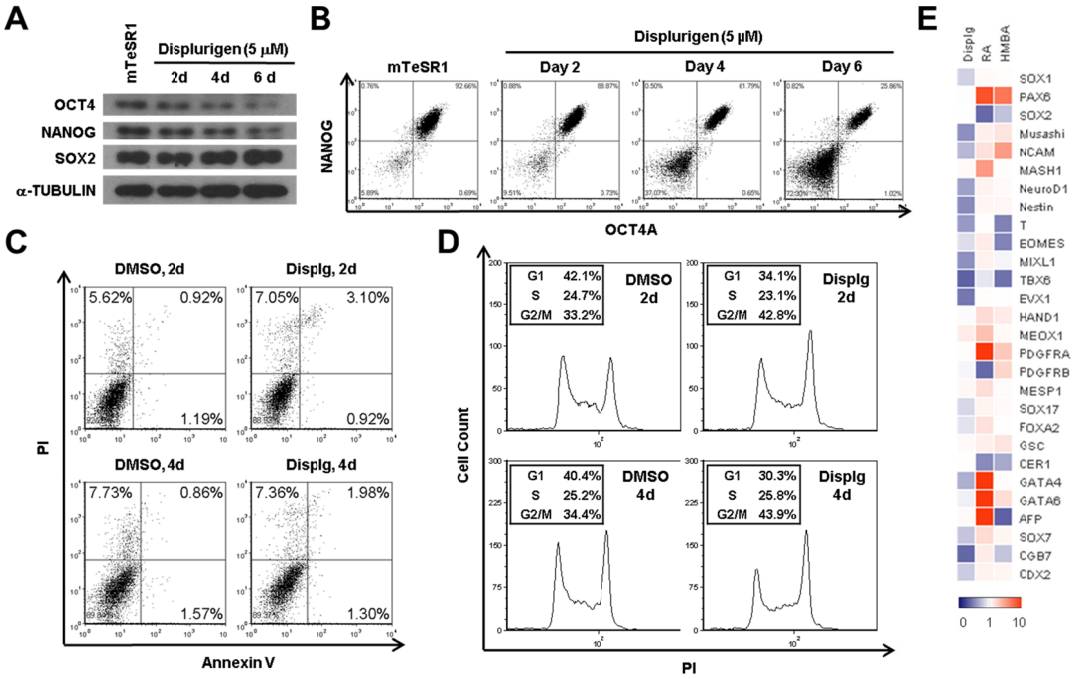

Figure S2, related to Figure 2. (**A**) Western blotting of OCT4, NANOG, and SOX2 in H1 hESCs untreated (mTeSR1) or treated with NSC375009 (Displurigen, 5 μM) for 2, 4, and 6 days (d). α-TUBULIN was used as a loading control. (**B**) Intracellular FACS analysis of OCT4A and NANOG in H1 hESCs untreated (mTeSR1) or treated with 5 μM NSC375009 (Displurigen) for 2, 4, and 6 days. (**C**) FACS analysis of propidium Iodide (PI) and Annexin V in H1 hESCs treated with DMSO or Displg (10 μM) for 2 days (2d) and 4 days (4d). (**D**) FACS analysis of PI in H1 hESCs treated with DMSO or Displg (10 μM) for 2 days (2d) and 4 days (4d). (**E**) Heatmap showing quantitative-PCR analysis of neuroectoderm (NE), mesoderm (MESO), endoderm (ENDO), and trophectoderm (TE) markers in H9 hESCs treated with Displg (10 μM), RA (10 μM), and HMBA (3 mM) for 6 days under differentiation condition. All values were normalized to the level (=1) of mRNA in DMSO control. Each bar represents mean ± SD (error bars). Overall average value of relative mRNA expression from n = 3 independent experiments were shown. *ACTB* (*β-actin*) was used as a loading control.

A

Hit Description	Score ($p < 0.05$ when score > 45)
keratin 1	278
keratin 10	179
heat shock 70 kDa protein 8 (HSPA8)	155

B

MSKGPAVGIDLGTTYSCVGVFQHG**KVEIIANDQGNRT**TPSYVAFTDTE**RLIGDA**
AKNQVAMNPTNTVFDAKRLIGRRFDDAVVQSDMKHWPFMVVNDAGRPKVQV
EYKGETKSFYPEEVSSMVLT**KMKEIAEAYLGKT**VTNAVVTVPAYFNDSQRQAT
KDAGTIAGLNVLRIINEPTAAAIAYGLDKKVGAERNVLIFDLGGGTFDVSILTIED
GIFEVKSTAGDTHLGGEDFDNRMVNHFIAEFKRKHKKDISENKRAVRRLRTAC
ERAKRTLSSSTQASIEIDSLYEGIDFYTSITRARFEELNADLFRGTLDPVEKALRD
AKLDKSQIHDIVLVGGSTRIPKIQ**KLLQDFFNGKE**LNKSINPDEAVAYGAAVQAA
ILSGDKSENVQDLLLLDVTPLSLGIETAGGVMTVLIK**RNTTIPTKQ**TQTFTTYSDN
QPGVLIQVYEGERAMTKDNNLLGKFELTGIPPAPRGVPQIEVTFDIDANGILNVS
AVDKSTGKENKITITNDKGRLSKEDIERMVQEAEKYKAEDEKQRDKVSS**KNSL**
ESYAFNMKATVEDEKLQGKINDEDKQKILDKCNEIINWLDKNQTAEKEEFEHQ
QKELEKVCNPIITKLYQSAGGMPGGMPGGFPGGGAPPSGGASSGPTIEEVD

C

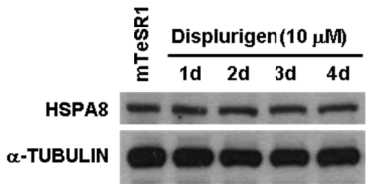

Figure S3, related to Figure 3. (**A**) List of all human proteins identified by mass spectrometry in the distinct 70 kDa band of Displg-biotin pull-down samples. (**B**) 7 unique peptide sequences in HSPA8 protein were identified by mass spectrometry. (**C**) Western blotting of HSPA8 in H1 hESCs untreated (mTeSR1) or treated with 10 μM Displg for 1 - 4 days (d). α-TUBULIN was used as a loading control.

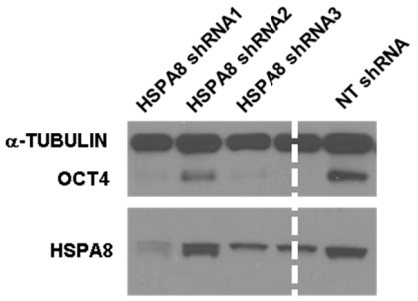

Figure S4, related to Figure 4. Western blotting of HSPA8-isoform-1 and OCT4 in H9 hESCs infected with lentivirus-particles containing Non-Target (NT) shRNA and HSPA8-1 shRNAs, shown as un-cropped blots. The lane which was cropped-off for Figure 4B is shown in this figure marked by a white dash line on top. The corresponding cropped blots are shown in Figure 4B.

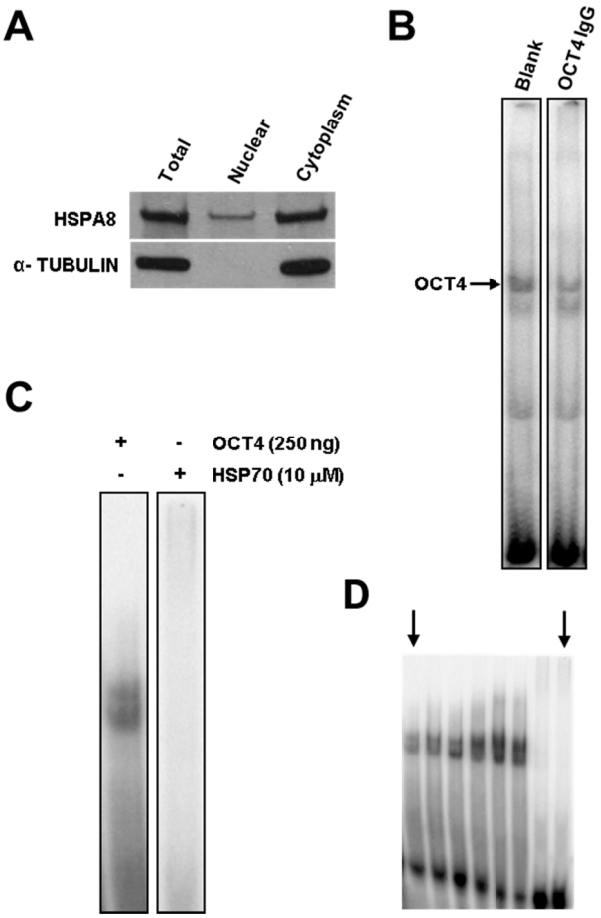

Figure S5, related to Figure 5. (**A**) Western blotting of HSPA8 in total lysate (Total), nuclear fraction (Nuclear), and cytoplasmic fraction (Cytoplasm) of undifferentiated H1 hESCs. Each lane was loaded with samples extracted from an equal number of cells. α-TUBULIN, an exclusively cytoplasmic protein, was used as a marker for the presence of cytoplasmic contents and to demonstrate clear separation of nuclear versus cytoplasmic fractions in this experiment. (**B**) EMSA using nuclear extracts of H9 hESCs treated with or without anti-OCT4 IgG showing the bindings of OCT4 proteins to the radio-labeled OCT4-binding element in *OCT4* promoter. The label "OCT4" points to the band sensitive to anti-OCT4 IgG treatment. (**C**) EMSA showing lack of DNA binding activity of purified recombinant HSP70 protein (10 μM) to a labeled OCT4-binding element *in vitro*. Purified recombinant OCT4 protein (250 ng) was used as a positive control. (**D**) The un-cropped image of Figure S5C. Black arrows point to the two lanes that were cropped and shown in Figure S5C.

Table S1. Antibody sources and dilutions

Antibody	Source	Catalog Number	Dilution
OCT4	Santa Cruz	sc-9081	1:1,000 (WB)
SOX2	Millipore	AB5603	1:500 (WB)
NANOG	Cell Signaling	4903P	1:500 (WB)
α-TUBULIN	Abcam	ab11304	1:10,000 (WB)
HSPA8-Isoform-I	R&D systems	MAB4148	1:100 (WB)
HSP70	Abcam	ab5439	1:1000 (WB)
OCT4A-Alexa647	BD Biosciences	562252	1:20 (FACS)
NANOG-PE	BD Biosciences	560483	1:5 (FACS)

(WB: Western blotting)

Table S2. qPCR primers

Primer Name	Forward Primer (5'-3')	Reverse Primer (5'-3')
ACTB	agagctacgagctgcctgac	cgtggatgccacaggact
OCT4 (isoform A)	cttctcgccccctccaggt	aaatagaacccccagggtgagc
NANOG	tttggaagctgctggggaag	gatgggaggaggggagagga
E-cadherin	tggaggaattcttgctttgc	cgctctcctccgaagaaac
N-cadherin	ctccatgtgccggatagc	cgatttcaccagaagcctctac
FN1	gacgcatcacttgcacttct	gcaggtttcctcgattatcct
SOX1	tacagccccatctccaactc	gctccgacttcaccagagag
PAX6	atttcccgctctggttcag	tagcgaagcctgacctctgt
SOX2	ggcagctacagcatgatgcaggagc	ctggtcatggagttgtactgcagg
Musashi	gagggttcgggtttgtcacg	ggcgacatcacctcctttgg
NCAM	atggaaactctattaaagtgaaccctg	tagacctcatactcagcattccagt
MASH1	cgacttcaccaactggttctg	atgcaggttgtgcgatca
NeuroD1	aagccatgaacgcagaggaggact	agctgtccatggtaccgtaa
Nestin	tccgatgggtttgcagat	cctcctcctgatcctcctct
T (Brachyury)	gctgtgacaggtacccaacc	catgcaggtgagttgtcagaa
EOMES	gtggggaggtcgaggttc	tgttctggaggtccatggtag
MIXL1	ggcgtcagagtgggaaatcc	gcagttcacatctacctcaagag
TBX6	gaacggcagaaactgtaagagg	gtgtgtctccgctcccatag
EVX1	ttcacccgagagcagattg	ccggttctggaaccacac
HAND1	aaaggccctacttccagagc	tgcgctgttaatgctctcag
MEOX1	aaagtgtcccctgcattctg	cactccagggttccacatct
PDGFRA	ccacctgagtgagattgtgg	tcttcaggaagtccaggtgaa
PDGFRB	aggctggccactacaccat	agcactcggacagggacat
MESP1	ctgttggagacctggatgc	cgtcagttgtcccttgtcac
SOX17	acgccgagttgagcaaga	tctgcctcctccacgaag
FOXA2	tgggagcggtgaagatggaagggcac	tcatgccagcgcccacgtacgacgac
GSC	gaggagaaagtggaggtctggtt	ctctgatgaggaccgcttctg
CER1	acagtgcccttcagccagact	acaactacttttttcacagccttcgt
GATA4	ggaagcccaagaacctgaat	gttgctggagttgctggaa
GATA6	aatacttcccccacaacacaa	ctctcccgcaccagtcat
AFP	agcttggtggtggatgaaac	ccctcttcagcaaagcagac
SOX7	ctcagggcagggaggtct	gcactcggataaggagagtcc
CGB7	tccttggcgctagaccac	cagggaggcacaggagtg
CDX2	gaccctcgccaccatgta	ctagggtacatgctcacgtcct

Table S3. shRNA sequences

Target	shRNA	Sequence (5' – 3')
HSPA8-1	HSPA8-1-1	ccgggcaactgttgaagatgagaaactcgagtttctcatcttcaacagttgctttttg
	HSPA8-1-2	ccggccaagacttcttcaatggaaactcgagtttccattgaagaagtcttggttttg
	HSPA8-1-3	ccgggcccgatttgaagaactgaatctcgagattcagttcttcaaatcgggctttttg

Table S4. EMSA probes

Probes	Forward Sequence (5'-3')	Reverse Sequence (5'-3')
NANOG	tctgcagctacttttgcattacaatggccttggtgag	ctcaccaaggccattgtaatgcaaaagtagctgcaga
OCT4	cagacagcagagagatgcatgacaaaggtgccgtgatggttc	gaaccatcacggcacctttgtcatgcatctctctgctgtctg
SOX2	gccgtttgccttcatttccataagaagattaaga	tcttaatcttcttatggaaatgaaggcaaacggc

SUPPLEMENTAL EXPERIMENTAL PROCEDURES

Cell culture

H9 and H1 hESC lines (WiCell Research Institute, Madison, WI) were maintained under a feeder condition or a feeder-independent condition. For the feeder condition (Thomson et al., 1998), primary mouse embryonic fibroblasts (MEFs) prepared from embryos of pregnant CF-1 mice (day 13.5 of gestation; Charles River) were cultured in Dulbecco's Modified Eagle Medium (DMEM) containing 10% FBS (Hyclone), 1% non-essential amino acids (NEAA; Invitrogen), and penicillin/streptomycin, and mitotically inactivated by gamma irradiation. H9 and H1 hESCs were cultured on irradiated MEFs in media containing DMEM/F12, 20% knockout serum replacement (KSR; Invitrogen), 4 ng/ml basic fibroblast growth factor (bFGF) (Invitrogen), 1% NEAA, 1 mM glutamine, and 0.1 mM β-mercaptoethanol. For the feeder-independent condition, hESCs were cultured on Matrigel (BD Biosciences)-coated plates in mTeSR1 medium (StemCell Technologies) as described (Ludwig et al., 2006). The experiments described in this study were conducted with H9 and H1 hESCs between passages 30 and 60. NTERA-2 cells (NTERA-2 cl.D1) were purchased from American Type Culture Collection (ATCC) and were cultured in Dulbecco's Modified Eagle's Medium (DMEM) containing 10% fetal bovine serum.

Generation and validation of NTERA-2-OP4k reporter cells

The plasmid containing EGFP driven by a fragment of OCT4 promoter (~4 kb) was kindly provided by Dr. Wei Cui (Imperial College London) and was as described (Gerrard et al., 2005). We established NTERA-2-OP4k cells containing the OCT4-EGFP construct by transfecting cells

using Amaxa Nucleofection System (Nucleofector Kit L; Program X-001), selecting transfected cells with G418 (500 μg/ml, 2 weeks), and enriching EGFP-positive cells using fluorescence-activated cell sorting (FACS) (Cytomation Plus, Dako).

For validation of reporter activity, NTERA-2-OP4k cells were plated at a density of 0.1 – 0.25 × 10^5 cells/cm^2 and incubated with RA (Sigma; 10 μM), HMBA (Sigma; 3 mM), bFGF (Invitrogen; 4 ng/ml), and Y-27632 (Calbiochem; 10 μM). After 6 - 7 days of incubation, changes in the level of EGFP signals were examined using fluorescent microscopy (Zeiss), flow cytometry (BD Biosciences LSR II), and fluorescent plate reader (Analyst HT, Molecular Devices).

Large-scale chemical screening

Large-scale chemical screening was conducted at the High-Throughput Screening Facility (HTSF) at the University of Illinois at Urbana−Champaign (http://www.scs.illinois.edu/htsf/index.html). The HTSF hosts 171,077 compounds from several compound libraries, which include the Marvel Library, the HTSF House Library, the ChemBridge MicroFormat Library, and the National Cancer Institute (NCI) library.

For large-scale chemical screening, NTERA-2-OP4k cells were trypsinized and seeded onto 96/384-well plates (at 0.1 – 0.25 × 10^5 cells/cm^2) using a WellMate Microplate Dispenser (Matrix). Compounds were added immediately after plating using a 96-well or a 384-well pin-tool. The first two and last two columns of 384-well plates and the first and last column of

96-well plates were used for DMSO treatment as negative controls. Cells were incubated for 6 - 7 days without medium change. EGFP expressions of individual wells were recorded by the fluorescence plate reader (Analyst HT, Molecular Devices). EGFP signal detected with compound treatments were compared to the DMSO control, and those with significant reduction (>30%; average level of background signals subtracted before comparison) were marked as potential hits and were subsequently inspected visually using a fluorescence microscope (Zeiss). The final compound concentrations applied to the screening plates were 5 - 10 μM (Marvel library), 500 nM - 1 μM (NCI library), 5 - 10 μM (House library), and 10 - 20 μg/ml (ChemBridge MicroFormat library).

Western blotting

Cultured cells were lysed directly by 2× Laemmli buffer (Bio-Rad), boiled for 5 min, and analyzed using SDS-PAGE electrophoresis followed by wet-transfer onto nitrocellulose membranes using a system manufactured by Bio-Rad. The membranes were blocked using blocking solution (5% BSA in Tris-buffered saline containing 0.1% Tween-20 [TBST]), and then incubated with primary antibodies, diluted in TBST, at 4°C overnight. The membranes were then washed by TBST for 3 × 5 min, and incubated with horseradish peroxidase (HRP) conjugated secondary antibodies at room temperature for 1 hr. Finally, the membranes were washed 5 min each time for 3 – 5 times by TBST and developed using Super-Signal West Pico Chemiluminescent Substrate (Pierce). Antibody information are described in Table S1.

RNA extraction, reverse transcription, and quantitative-PCR

Total RNA were isolated using RNeasy mini kit (QIAGEN). cDNAs were synthesized from the purified RNAs using Reverse Transcription System (Promega). Quantitative-PCR was performed using QuantiTech SYBR Green PCR kit (QIAGEN). Signals were analyzed using the comparative C_T method, and ACTB gene was used as an internal control. The designs of gene-specific primers are described in Table S2.

Intracellular FACS analysis

Single cell suspensions were acquired through Accutase (Invitrogen) treatment. Cells were fixed and stained using Transcription Factor Buffer Set (BD Biosciences) following the manufacturer's instructions. Conjugated antibodies including OCT4A-Alexa647 and NANOG-PE (Table S1) were used. Cells were resuspended in PBS supplemented with 1% BSA and analyzed using a BD Biosciences LSR II flow cytometry analyzer and BD FACSDiva software.

Apoptosis analysis

Cells were collected and washed in cold PBS. Cells were then stained using FITC Annexin V Apoptosis Detection Kit I (BD Biosciences) following the manufacturer's instructions. Cells were analyzed using a BD BD Biosciences LSR II flow cytometry analyzer and BD FACSDiva software.

Cell cycle analysis

Cells were collected and washed in cold PBS, and fixed in chilled ethanol overnight at 4°C. Cells were then washed and resuspended in PBS with 50 μg/ml propidium iodide (PI) and 100 μg/ml RNase A for 30 min at 37°C. DNA content was measured by flow cytometry.

Differentiation assay

H9 and H1 hESC were seeded onto Matrigel coated plates in single cell in mTeSR1 medium. Cells were then incubated with a basal differentiation medium containing Advanced RPMI 1640 (Invitrogen), 2% B-27 supplement (Invitrogen), and 1% Glutamax (Invitrogen) with compound treatments (DMSO, 10 μM Displg, 10 μM RA, and 3 mM HMBA). Medium was changed every other day. Samples were collected on day 6 for analysis.

Synthesis of Displurigen-biotin

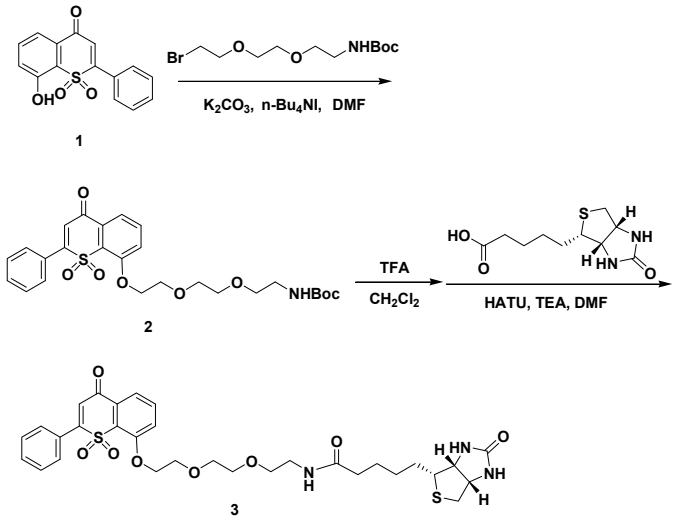

Synthesis of Compound 2: Compound 1 (0.0055 g, 0.019 mmol), 2-[2-(2-tertbutoxycalbonyl

aminoethoxy) ethoxy]ethyl bromide (0.0071 g, 0.023 mmol), K_2CO_3 (0.0030 g, 0.022 mmol) and *n*-Bu_4NI (0.0014 g, 0.0038 mmol) were suspended in DMF (1 mL). The suspension was heated at 60 °C for 12 h. After evaporation of the solvent, crude product was purified by flash chromatography on silica gel (EtOAc : Hexanes = 1 : 1) and then EtoAc to give **2** as solid (0.0086 g, 0.0166 mmol, 86.5 %). ^{1}H NMR (300MHz, $CDCl_3$, 25 ^{o}C) δ 1.43 (s, 9H), 3.29 (m, 2H), 3.53 (t, *J* = 5.1 Hz, 2H), 3.58 (m, 2H), 3.76 (m, 2H), 3.99 (t, *J* = 4.5 Hz, 2H), 4.40 (t, *J* = 4.8 Hz, 2H), 4.98 (bs, 1H), 6.73 (s, 1H), 7.42-7.62 (m, 4H), 7.68 (t, *J* = 6.9 Hz, 1H), 7.83-7.90 (m, 3H); ^{13}C NMR (75 MHz, $CDCl_3$, 25 ^{o}C) 28.4, 40.4, 69.3, 70.2, 70.4, 70.5, 71.4, 119.9, 120.4, 127.8, 129.1, 130.0, 131.6, 133.8, 154.5, 155.9, 156.6, 178.4

Synthesis of Compound 3: Deprotection of **2** (0.0086 g, 0.0166 mmol) was performed with 0.5 mL of CH_2Cl_2 and 0.2 mL TFA at 0 °C. After stirring at 0 °C for 3 h, the reaction mixture was concentrated. Toluene (0.5 mL) was added to the residue and then evaporated to remove TFA. The procedure was repeated three times. The resulting TFA salt of the deprotected amine was dissolved in DMF (1 mL) and D-biotin (0.0071 g, 0.029 mmol). HATU (0.012 g, 0.0316 mmol) was added followed by a triethylamine (25 μL, 0.18 mmol). After stirring at rt overnight, the mixture was concentrated under reduced pressure and the residue was purified by flash chromatography on silica gel ($CHCl_3$: EtOH = 10 : 1), which gave **3** (0.0077 g, 0.012 mmol, 72.1 %) as solid. ^{1}H NMR (300 MHz, $CDCl_3$, 25 °C) δ 1.37 (m, 2H), 1.68 (m, 4H), 2.15 (t, *J* = 7.5 Hz, 2H), 2.70 (d, *J* = 12.9 Hz, 1H), 2.88 (dd, *J* = 5.4 Hz, *J* = 12.9 Hz, 1H), 3.09 (m, 1H), 3.40 (m, 2H), 3.56 (t, *J* = 5.1 Hz, 2H), 3.67 (m, 2H), 3.78 (m, 2H), 3.98 (t, *J* = 4.8 Hz, 2H), 4.23 (m,

1H), 4.40 (m, 2H), 4.47 (m, 1H), 4.93 (s, 1H), 5.77 (s, 1H), 6.50 (t, 1H), 6.75 (s, 1H), 7.42-7.60 (m, 4H), 7.66 (t, J = 7.5 Hz, 1H), 7.84 (m, 3H); ^{13}C NMR (75 MHz, $CDCl_3$, 25 ^{o}C) 25.8, 28.3, 36.1, 39.4, 40.8, 55.7, 60.4, 62.0, 69.4, 70.2, 70.6, 70.7, 71.2, 120.0, 120.7, 128.2, 129.4, 130.3, 131.9, 134.2, 154.6, 156.7, 164.0, 173.5, 178.6; MS (ESI^+) (m/z): $[M + H]^+$ Calcd. For $C_{31}H_{38}N_3O_8S_2$: 644.2095; Found: 644.2104.

Affinity chromatography, electrophoresis, and silver staining

hESCs were cultured under the feeder-independent condition with or without the presence of displurigen-biotin (10 μM) overnight, washed in PBS three times and lysed in Ice-cold RIPA buffer supplemented with protease and phosphatase inhibitors cocktail (Sigma). The lysates were then diluted two-fold by Tris buffer (50 mM Tris-HCl, pH 7.5).

For affinity chromatography ("pull-down"), diluted lysates were incubated with streptavidin−agarose beads (Sigma) for 5 hr at 4°C. The beads were collected using centrifugation and washed with wash buffer (75 mM NaCl, 0.5 mM EDTA, 0.5% Triton X-100, 0.5% sodium deoxycholate, 0.05% SDS, 50 mM Tris-HCl, pH 7.6). The washed beads were suspended in 2× Laemmli buffer (Bio-Rad) and heated at 100°C for 5 min.

For electrophoresis and silver staining, 10 μl samples were loaded on polyacrylamide gel. Silver staining was performed using ProteoSilver Plus Silver Stain Kit (Sigma). Protein bands detected by silver staining were selectively excised for mass spectrometry analysis.

Mass spectrometry analysis

Gel slices were dehydrated and destained in 50% Acetonitrile + 25 mM NH4HCO3 and gently crushed using a plastic pestle inside a 1.5 ml eppendorf tube. The crushed gel was dried briefly using Speedvac (Thermo) before digestion with Trypsin (mass spectrometry grade, G-Biosciences at 1:50 w/w) in 25 mM ammonium bicarbonate. Digestion was performed using a CEM Discover Microwave Digestor (Mathews, NC) for 15 min at 75 watts, 55°C. The digested peptides were extracted using 50% acetonitrile and 5% formic acid, lyophilized and reconstituted in 5% acetonitrile and 0.1% formic, 10 µl of which was used for LC/MS analysis. Mass spectrometry was performed using a Waters Q-ToF connected to a Waters nanoAcquity UPLC (Milford, MA). Column was a Waters Atlantis dC18 nanoAcquity UPLC column 75 µm x 150 mm (3 µm particle size) running at 250 nl/min. Gradient was from 100% A to 60% B (A: water and 0.1% formic acid; B: acetonitrile and 0.1% formic acid). Data collection was performed using MassLynx 4.1 (Waters). The top 4 intensive precursor ions from each survey scan were subjected to MS/MS by Collision Induced Dissociation (CID). The raw mass spectrometric data were processed using ProteinLynx Global Server 2.2.5 (Waters). The refined peaklists were analyzed using Mascot 2.2 (Matrix Science, London, UK) with a tolerance of ± 0.4 Da for both the precursor ions and fragment ions. Searches were carried out using the NCBI non-redundant protein database.

Embryoid body (EB) formation

H9 and H1 hESC colonies were dissociated from the culture surface by 20 min treatment of Dispase (Invitrogen). Suspended colonies were pooled by brief centrifugation (1000 rpm, 1 min),

resuspended in medium containing Advanced RPMI 1640 (Invitrogen), 2% B-27 supplement (Invitrogen), and 1% Glutamax (Invitrogen), and then plated into ultra-low attachment plates (Corning). Medium was changed every other day.

***In vitro* ATPase assay**

The HSP70 ATPase rates were determined as described (Freeman et al., 1995). In brief, ATP hydrolysis was determined by measuring the release of [^{32}P]Pi from [γ-^{32}P]ATP. The ATPase rates were calculated utilizing an average [γ-^{32}P]ATP hydrolysis rate at each time point (5, 10, 15 and 20 min) from three separate experiments after the background hydrolysis was subtracted. The data were visualized and quantified by PhosphorImager analysis (Molecular Dynamics). The effect of Displurigen on the ATPase rate of HSP70 was measured by incubating HSP70 (5 min) with varying levels of Displurigen prior to the introduction of ATP.

Lentivirus production and infection

For viral packaging, expression vectors were co-transfected with pCMV-dR8.91 and pCMV-VSV-G into 293T cells by $CaPO_4$ precipitation. After overnight incubation, culture medium was replaced by virus-packaging medium containing DMEM, 30% FBS, and 1 mM sodium pyruvate. Supernatants were collected 48 hr later and concentrated approximately 100× by ultracentrifuge (20,000 rpm, 1 hr). H1 and H9 hESCs were infected by virus concentrates in the presence of Polybrene (6 μg/ml), and then subjected to puromycin (0.5 μg/ml) selection for 3-5 days prior to analysis.

HSPA8 overexpression plasmid construction

HSPA8-isoform-1 cDNA clone was purchased from OriGene (SC322471), and subcloned into a pSin-EF2 plasmid (Addgene; modified with a short adaptor sequence) at the MluI/NdeI site.

Immunoprecipitation

Cells treated with DMSO or Displg (100 μM, 2 hours) were lysed in ice-cold RIPA buffer (Pierce) supplemented with a protease inhibitor cocktail (Sigma). After clarification, cell lysates were pre-cleared with Protein A/G magnetic beads (Pierce) and thereafter incubated with 2 μg of anti-OCT4 antibody (Santa Cruz) and with DMSO or 1 mM Displg, respectively. After 2 hours of incubation at 4°C, Protein A/G magnetic beads were added to the cell lysates. The resulting immunoprecipitates were washed with ice-cold PBS and analyzed by Western blotting.

Electrophoretic mobility shift assay (EMSA)

EMSA analysis was performed using Buffer C nuclear extracts (10 μg) from hESCs. The extracts were incubated with poly dI-dC (Sigma) and ^{32}P-end labeled oligonucleotides: *OCT4*, *NANOG* and *SOX2* binding sequence probes along with the complimentary primers. The protein-DNA complexes were resolved by native polyacrylamide gel (4%) electrophoresis and the dried gels were visualized using a PhosphorImager (Molecular Dynamics). Sequences of *OCT4*, *NANOG* and *SOX2* probes are listed in Table S4.

In vitro OCT4-DNA binding assay

OCT4 cDNA was cloned from the pSin-EF2-OCT4-Pur vector (Addgene) and inserted into the PET-24a protein expression vector, which contains a C-terminal His Tag. OCT4 and HSP70 proteins were expressed in Rosetta cells and captured with the Talon metal affinity resin (Clontech). The proteins were further purified using Resource Q and Superdex 200 columns (GE Healthcare). OCT4 protein binding to the *OCT4* response element (Supplemental Experimental Procedures) was assessed by the use of EMSA analysis in the presence or absence of purified HSP70 protein.

Statistical analysis

Statistical analyses were performed using Microsoft Excel. Student's *t*-test was used to compare two experimental groups, assuming unequal variances. Differences are considered significant when $p < 0.05$.

SUPPLEMENTAL REFERENCES

Freeman, B.C., Myers, M.P., Schumacher, R., and Morimoto, R.I. (1995). Identification of a Regulatory Motif in Hsp70 That Affects Atpase Activity, Substrate-Binding and Interaction with Hdj-1. Embo J *14*, 2281-2292.

Gerrard, L., Zhao, D., Clark, A.J., and Cui, W. (2005). Stably transfected human embryonic stem cell clones express OCT4-specific green fluorescent protein and maintain self-renewal and pluripotency. Stem Cells *23*, 124-133.

Ludwig, T.E., Levenstein, M.E., Jones, J.M., Berggren, W.T., Mitchen, E.R., Frane, J.L., Crandall, L.J., Daigh, C.A., Conard, K.R., Piekarczyk, M.S.*, et al.* (2006). Derivation of human embryonic stem cells in defined conditions. Nat Biotechnol *24*, 185-187.

Thomson, J.A., Itskovitz-Eldor, J., Shapiro, S.S., Waknitz, M.A., Swiergiel, J.J., Marshall, V.S., and Jones, J.M. (1998). Embryonic stem cell lines derived from human blastocysts. In Science, pp. 1145-1147.